PROCEEDINGS of ISMA 2019
International Symposium on Music Acoustics

13 - 17 September 2019 in Detmold, Germany

Computational aeroacoustic modeling of single-reed mouthpiece using Palabos

Song WANG *, Gary SCAVONE †

Computational Acoustic Modeling Laboratory (CAML),
Centre for Interdisciplinary Research in Music Media and Technology (CIRMMT),
Schulich School of Music, McGill University, Canada

Abstract

The sound generation behavior of a single-reed instrument can be determined from its aeroacoustic characteristics. Computational aeroacoustics (CAA) modeling offers a mean to analyze the aeroacoustics behavior of such a system. The lattice Boltzmann method (LBM) models fluid on a mesoscopic level and has certain advantages over traditional Navier-Stokes approaches in solving CAA problems. In this study, we present results from an aeroacoustic analysis of a 2D single-reed mouthpiece system using an open-source, parallelized lattice Boltzmann solver called Palabos. A variety of functionalities and components are investigated, including the parallelization, the moving boundary, and the non-reflecting boundary condition, which demonstrates the versatility of Palabos. Different mouthpiece geometries are tested with both static and moving reeds. The nonlinear characteristics of the mouthpiece-reed system derived from this study are then compared with the theoretical quasi-static flow model.

Keywords: Computational aeroacoustics, Single-reed mouthpiece, Lattice Boltzmann method

1 INTRODUCTION

Wind instruments can generally be decomposed into two components, the sound resonator, and the sound generator. For a single-reed instrument, the sound generator corresponds to its nonlinear mouthpiece-reed system that largely determines the dynamics of the whole instrument. The mouthpiece-reed system is generally analyzed in terms of a nonlinear relationship between the volume flow rate and the pressure difference across the reed channel.

The flow through the reed channel was initially assumed to be frictionless, incompressible, and quasi-stationary so that the mouthpiece-reed system can be modeled based on the Bernoulli equation [1]. Hirschberg et al. (1990) [2] improved the model by introducing viscous effects while keeping the incompressible and quasi-static approximation. The reed channel of the mouthpiece is modeled as a two-dimensional Borda tube. The flow separation at the reed channel entrance is taken into account by introducing the vena contracta coefficient ($0.5 < \alpha \leq 0.611$). For a larger Reynolds number and a longer channel, the flow will reattach in the reed channel, and the flow after the reattachment point is approximated by the Poiseuille flow. Van Zon et al. (1990) [3] further extended this model by replacing the Bernoulli flow by the boundary layer flow to represent the flow in between the separation point at the entrance and the reattach point in the reed channel. The Van Zon model is validated by measurements with a static reed [3]. However, the quasi-stationary approximation fails in dynamic flow even though the estimated Strouhal number is much smaller than one [3]. Discrepancies of the vena contracta coefficient are also found when comparing the theoretical value to both the measurement [4, 5] and the numerical simulation results [6, 7].

In this paper, the dynamic behavior of the single-reed mouthpiece-reed system is studied using Palabos [8], an open-source computational fluid dynamics solver based on the lattice Boltzmann method (LBM). In contrast with traditional Navier-Stokes (NS) solvers, LBM is a mesoscopic method based on the discretization of the Boltzmann equation and has been proven to perform well in solving aeroacoustic problems [9, 10, 11]. In order to model the mouthpiece-reed system of a single-reed instrument, different algorithms are used including the

*song.wang5@mail.mcgill.ca
†gary.scavone@mcgill.ca

multi-block technique for parallelization, the non-reflecting boundary condition [12], and the immersed boundary method (IBM) for building the off-grid boundary and the moving boundary [13].

This paper is organized as follows: Section 2 presents the basic LBM scheme and different algorithms used in the simulation. The details of the simulation setup are described as well. The numerical results of the static reed case and their comparison with the theoretical solution are discussed in Section 3. A preliminary moving reed test is also presented. Finally, a conclusion is given in Section 4.

2 NUMERICAL PROCEDURE

2.1 Lattice Boltzmann method

The lattice Boltzmann method (LBM) is a numerical method based on the lattice Boltzmann equation (LBE) that is obtained by discretizing the Boltzmann equation in physical space, velocity space and time, given as

$$f_i(\boldsymbol{x} + \boldsymbol{e}_i \Delta t, t + \Delta t) = f_i(\boldsymbol{x}, t) + \Omega_i(\boldsymbol{x}, t), \tag{1}$$

where f_i is the distribution function, $\{e_i\}$ is the discrete velocity set, Δt is the time step that usually equals 1, and $\Omega(\boldsymbol{x}, t)$ is the collision operator. The D2Q9 model is used in this paper, which discretizes the velocity space into nine directions for a two-dimensional space. The lattice sound speed is defined as $c_s = 1/\sqrt{3}$, the weight coefficients $\{w_i\}$ are set as

$$w_i = \begin{cases} \frac{4}{9}, & i = 0, \\ \frac{1}{9}, & i = 2, 4, 6, 8, \\ \frac{1}{36}, & i = 1, 3, 5, 7, \end{cases} \tag{2}$$

and $\boldsymbol{e}_i$ is given as

$$\boldsymbol{e}_i = \begin{cases} (0, 0), & i = 0, \\ (\cos\frac{(i+2)\pi}{4}, \sin\frac{(i+2)\pi}{4}), & i = 2, 4, 6, 8, \\ \sqrt{2}(\cos\frac{(i+2)\pi}{4}, \sin\frac{(i+2)\pi}{4}), & i = 1, 3, 5, 7. \end{cases} \tag{3}$$

One of the most widely used collision operators is known as Bhatnagar-Gross-Krook (BGK),

$$\Omega_i(\boldsymbol{x}, t) = -\frac{1}{\tau}(f_i - f_i^{\mathrm{eq}})\Delta t, \tag{4}$$

where τ is the relaxation time related to the kinematic viscosity $\nu = c_s^2(\tau - \frac{\Delta t}{2})$, and f_i^{eq} is the equilibrium distribution function given by

$$f_i^{\mathrm{eq}}(\boldsymbol{x}, t) = w_i \rho \left(1 + \frac{\boldsymbol{u} \cdot \boldsymbol{e}_i}{c_s^2} + \frac{(\boldsymbol{u} \cdot \boldsymbol{e}_i)^2}{2c_s^4} - \frac{\boldsymbol{u} \cdot \boldsymbol{u}}{2c_s^2}\right) \tag{5}$$

The macroscopic density and velocity are found as $\rho = \sum_i f_i$ and $\boldsymbol{u} = \sum_i \boldsymbol{e}_i f_i / \rho$, respectively. Based on the isothermal condition, the pressure p can be determined by $p = \rho c_s^2$.

Despite the simplicity of the original BGK scheme, it can be unstable for high Mach number and high Reynolds number flow. Spurious waves due to the numerical error might also disturb the acoustic field. In order to achieve a better solution, the recursive regularized BGK (rrBGK) LBM is applied in this paper. The rrBGK was first introduced to increase the stability and accuracy by Malaspinas [14] for isothermal and weakly compressible flow, based on the original regularized BGK proposed by Latt and Chopard [15]. Coreixas et al. [16] further generalized it for thermal and fully compressible flow. The rrBGK starts by expressing the distribution function f as the sum of the equilibrium distribution f^{eq} and the non-equilibrium part f^{neq} based on the Chapman-Enskog expansion

$$f = f^{\mathrm{eq}} + f^{\mathrm{neq}}. \tag{6}$$

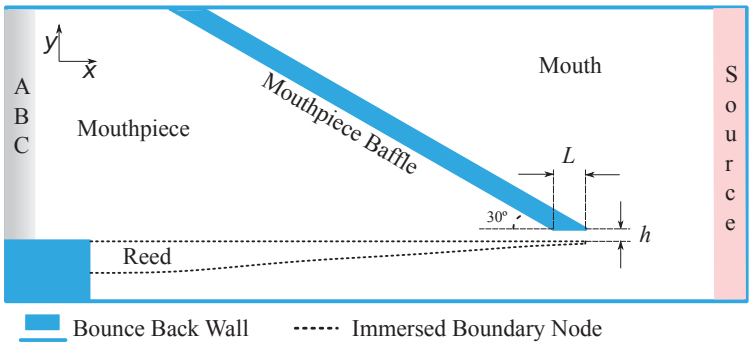

Figure 1. The schematic view of the computational domain

Then, both f^{eq} and f^{neq} can be expressed in terms of Hermite polynomials whose coefficients can be calculated recursively. Further details of the algorithms can be found in the paper by Malaspinas [14].

2.2 Simulation setup

A simplified two-dimensional mouthpiece is set up in the fluid domain as shown in Figure 1. The size of the domain is 5×2 cm^2 with the spatial grid size of $\Delta x = 8 \times 10^{-5}$m. The time step is set as $\Delta t = 1.35 \times 10^{-7}$s. The lattice relaxation time is $\tau = 0.5098$, corresponding to the physical kinematic viscosity of $\nu = 1.55 \times 10^{-4}$m^2/s, which is an order of magnitude larger than the air kinematic viscosity.

The absorbing boundary condition (ABC) proposed by Kam et al. [12] is applied at the exit of the mouthpiece (left side of Figure 1) to get rid of the acoustic feedback. The same algorithm is used at the inlet with a non-zero flow and pressure target, working as the pressure source [17]. The immersed boundary method [13] is implemented in Palabos for modeling the reed, which allows the off-lattice boundary and the moving boundary conditions. The one-dimensional distributed model [18] is used for modeling the reed as well as the reed-mouthpiece interaction. Different from previous LBM simulations [6, 7], the reed thickness is introduced into the model. For the fixed walls of the mouthpiece, the bounce-back scheme is used for a no-slip flow condition.

In Palabos, the parallelization is performed with the message-passing interface (MPI). By using the multi-block technique, the computational domain is divided into multi-blocks and are assigned to different processors. As well, the one-side communication technique is used for distributing the reed information to different processors. All the simulations were run on the Compute Canada CPU cluster (Intel E5-2683 v4 Broadwell @ 2.1GHz) with 32 processors.

For this study, we intended to apply the grid refinement technique to improve the simulation efficiency. With such a scheme, the finest grid could be deployed around the reed channel to help better capture the flow properties. However, the problem becomes complex due to the interaction between the off-lattice boundary and the moving boundary across regions of different resolution. So, even though the grid refinement has already been implemented [19] in Palabos and tested in other aeroacoustic simulations [10], its application in our wind instrument model is left for a future investigation.

3 RESULTS

3.1 Static Reed Results

In the static reed case, two different mouthpiece profiles with different channel lengths ($L/h = 1$ and $L/h = 4$) are studied, where L stands for the reed channel length and $h = 1.3$ mm represents the channel height. The simulation lasts for 500,000 iterations in total. The mouth pressure starts from 0 Pa and linearly increases to

11 kPa within 200,000 iterations, and holds for 50,000 iterations. It then decreases back to zero within the next 200,000 iterations and holds there until the end of the simulation. The mouth pressure p_{mouth} is measured by averaging a rectangular field in between the top and bottom domain boundaries, starting from the tip of the mouthpiece to the left of pressure source buffer. The flow volume rate U_{jet} is calculated by multiplying the cross-section area by the averaged flow velocity measured across the end of the reed channel. The pressure p_{jet} is measured by taking the average of the pressure over the cross-section area at the end of the reed channel. The pressure difference is defined as $\Delta p = p_{mouth} - p_{jet}$.

Simulation results and the comparison with the theoretical results [3] are shown in Figure 2 and Figure 3. Four different plots are shown to better explain the results, including the Δp - U_{jet} plot, the Δp - α plot, the pressure/flow history plot, and the Re - α plot. The Re - α plot only includes the first half of the simulation, i.e., 250,000 iterations.

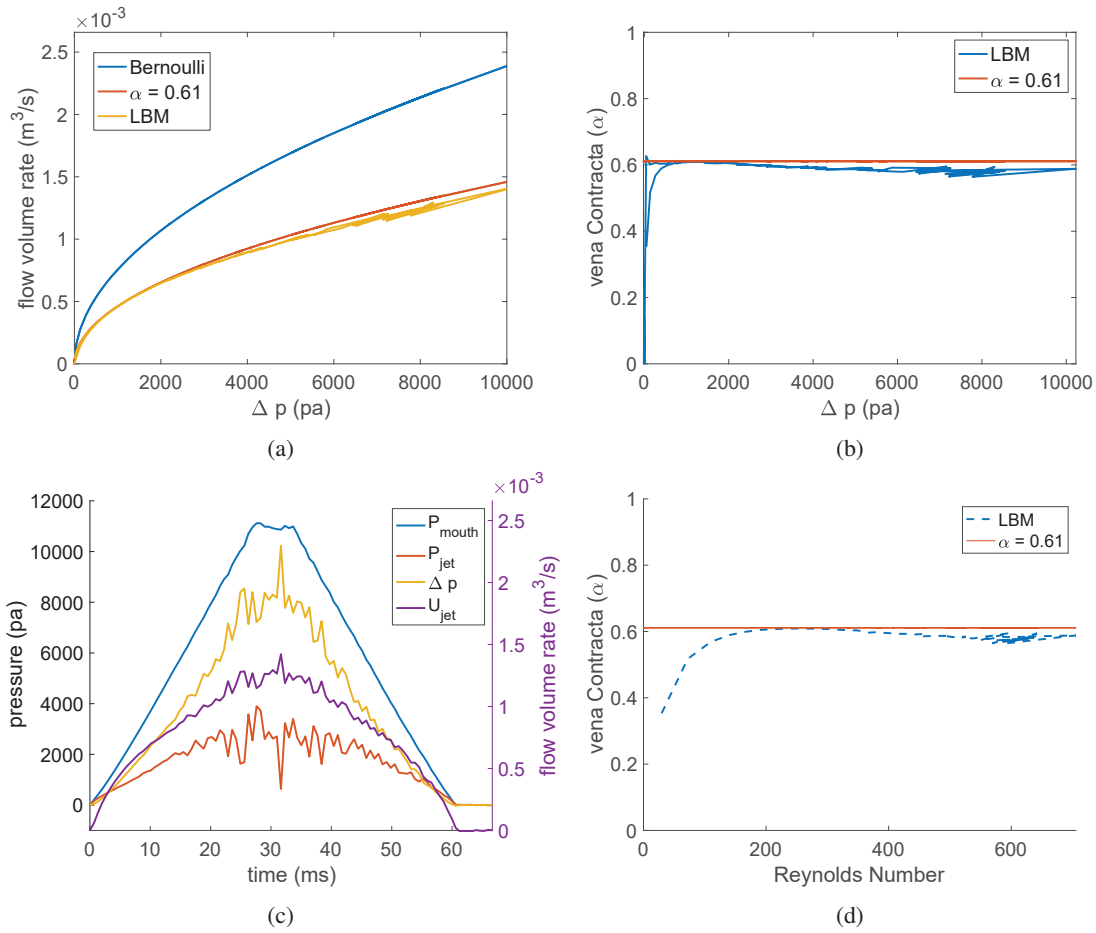

Figure 2. The LBM simulation results for the mouthpiece with $L/h = 1$.

For the short reed channel mouthpiece ($L/h = 1$), the simulation result matches the theoretical estimation very well and the calculated vena contracta coefficient α falls into the theoretical range $(0.5, 0.611]$ as proposed by Hirschberg et al. 1990 [2]. However, for the long reed channel mouthpiece ($L/h = 4$), instead of being comparable with the van Zon model for long reed channel, the LBM flow is more similar to the short reed channel flow with a slightly lower α. Similar results were also observed by Shi et al. [6], who attributed them to the large viscosity used in LBM. In order to test this explanation, the mouthpiece with a more realistic kinematic

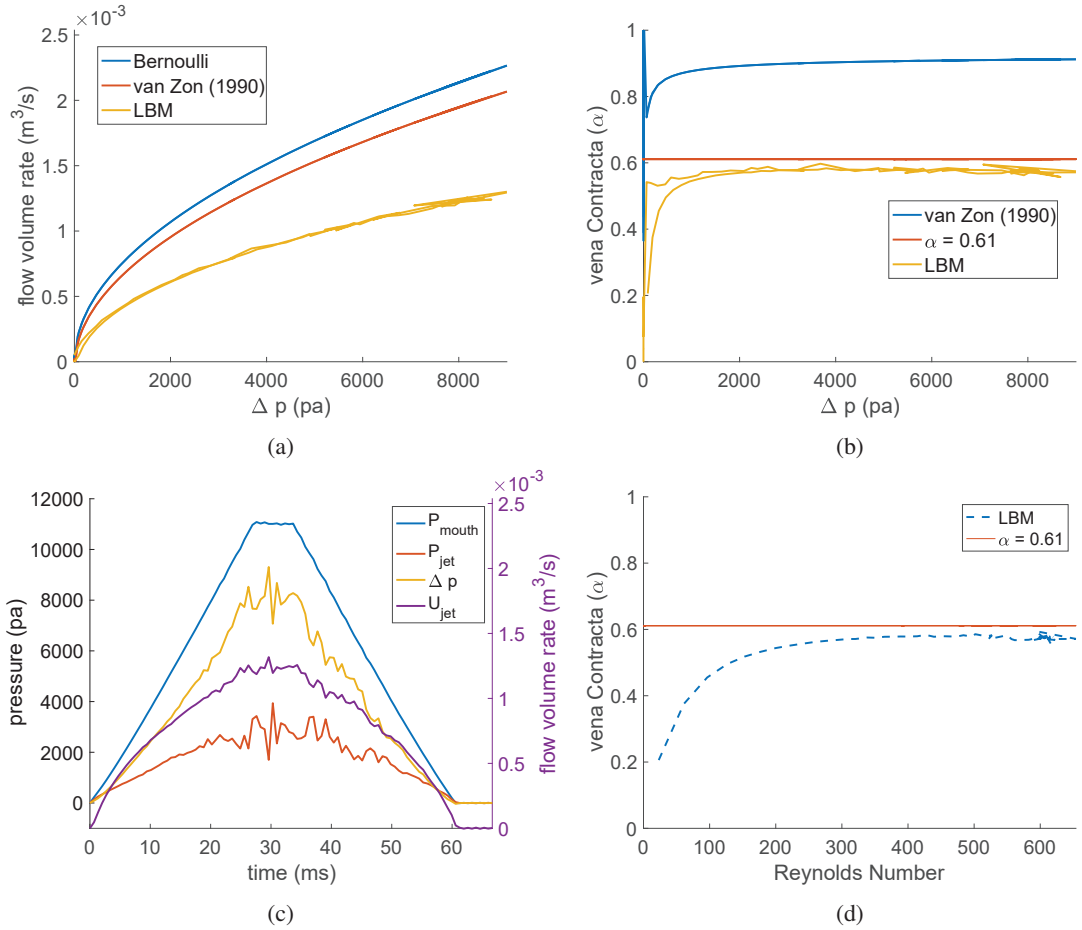

Figure 3. The LBM simulation results for the mouthpiece with $L/h = 4$.

viscosity ($\nu = 4.75 \times 10^{-5} \mathrm{m}^2/\mathrm{s}$) flow is simulated with finer grids ($\Delta x = 4.25 \times 10^{-5} \mathrm{m}$). As shown in Figure 4, decreasing the viscosity does help increase the flow rate a little bit. However, the flow becomes more turbulent as the Reynolds number increases.

3.2 Moving Reed Results

In this section, a simulation with a moving reed is presented. The pressure difference between the top and bottom of each immersed boundary node of the reed is taken as the external force that drives the reed to move. The velocity of each node is then used in the immersed boundary method. The target pressure of the source buffer is set as 8kPa. The mouth pressure, the jet volume flow rate, and the jet pressure are measured at the same position as discussed in the previous section. In addition, the mouthpiece pressure at the downstream of the mouthpiece, near the absorbing boundary layer, is also measured. All the results, together with the tip displacement, are shown in Figure 5. In this preliminary simulation setup, the system does not achieve a steady-state regime but instead decays over time. The volume flow rate appears to be noisy, which might be due to the low grid resolution. For example, when the reed tends to close, there could be only one grid point for calculating the volume flow rate, which is insufficient. Despite this, the result shows the ability of the framework to simulate the fully coupled fluid-structure interaction problem.

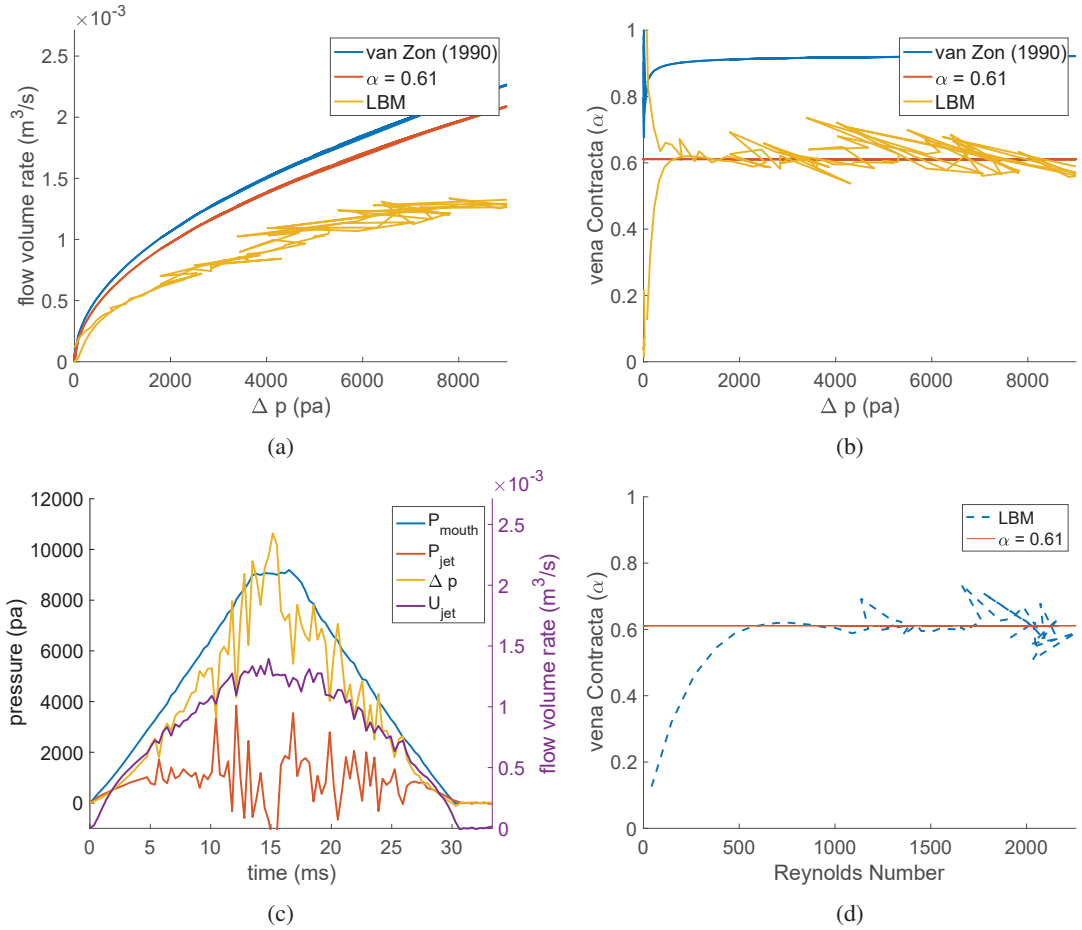

Figure 4. The LBM simulation results for the mouthpiece with $L/h = 4$ with the kinematic viscosity of $\nu = 4.75 \times 10^{-5} \mathrm{m}^2/\mathrm{s}$.

4 CONCLUSIONS

In this paper, a single-reed mouthpiece reed system is modeled within Palabos. Different functionalities have been tested. For the static reed simulation, the results of the short reed channel show a good agreement with the theoretical model. However, for a longer reed channel mouthpiece, a large discrepancy is found between the LBM simulation and the van Zon model. Though it is partially due to the high kinematic viscosity used in the simulation, it might also be caused by the relative larger numerical dissipation of the MRT or the rrBGK scheme that helps maintain the stability. In addition, as shown in the pressure/flow history plots and the Re - α plots, the flow starts to get turbulent as the pressure goes higher. Such turbulent behavior that happens in the simulation might be another reason for the discrepancy. However, considering the Reynolds number is still much smaller than 4000, further experiments is need to judge if this behavior is a physical turbulence or the numerical noise.

For the moving reed simulation, a preliminary result is presented, which shows the ability of the framework in solving the fully coupled fluid-structure interaction problem. However, the low-resolution and first-order IBM might be insufficient for complicated cases, such as the flow that involves the collision of the reed with the mouthpiece. In such case, a high-order of IBM and grid refinement should be implemented. In addition, impedance acoustic boundary condition is also needed to study the fluid-acoustic-solid interaction in

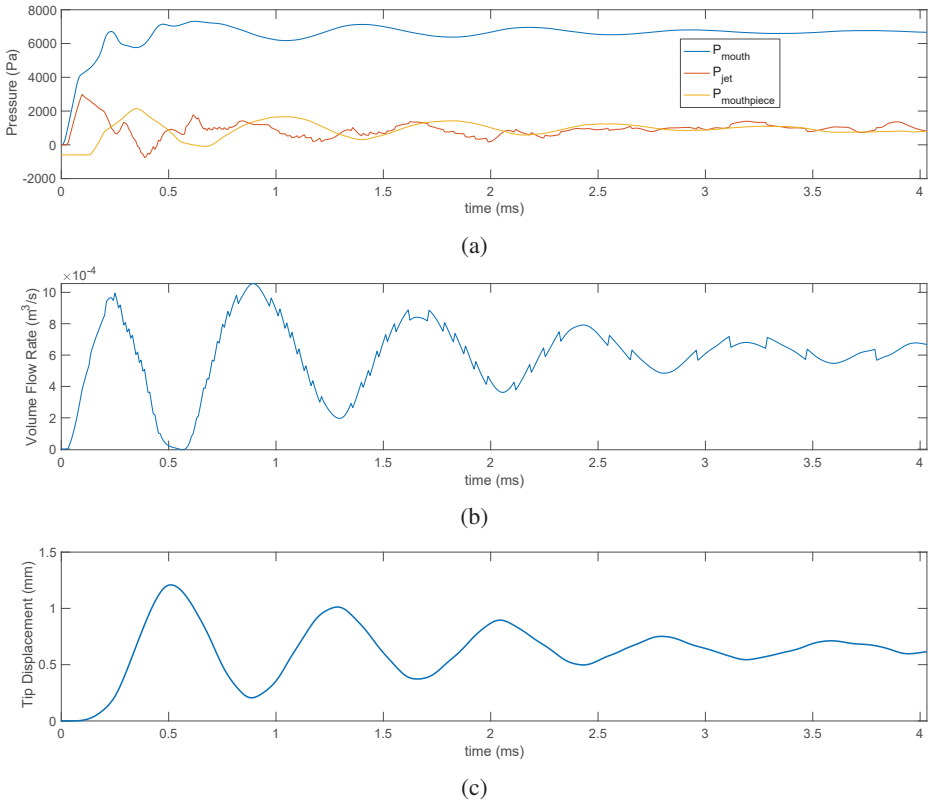

Figure 5. The moving reed simulation result.

the mouthpiece-reed system.

ACKNOWLEDGEMENTS

The authors wish to acknowledge the support from Natural Sciences and Engineering Research Council of Canada, and the Centre for Interdisciplinary Research in Music Media and Technology at McGill University. The authors also acknowledge the compute resources provided by Compute Canada.

REFERENCES

[1] John Backus. Small-Vibration Theory of the Clarinet. *The Journal of the Acoustical Society of America*, 35(3):305–313, 1963.

[2] A. Hirschberg, R. W. A. Van de Laar, J. P. Marrou-Maurieres, A. P. J. Wijnands, H. J. Dane, S. G. Kruijswijk, and A. J. M. Houtsma. A quasi-stationary model of air flow in the reed channel of single-reed woodwind instruments. *Acta Acustica united with Acustica*, 70(2):146–154, 1990.

[3] J. Van Zon, A. Hirschberg, J. Gilbert, and A. P. J. Wijnands. Flow through the reed channel of a single reed music instrument. *Le Journal de Physique Colloques*, 51(C2):C2–821, 1990.

[4] Jean-Pierre Dalmont, Joël Gilbert, and Sébastien Ollivier. Nonlinear characteristics of single-reed instru-

ments: Quasistatic volume flow and reed opening measurements. *The Journal of the Acoustical Society of America*, 114(4):2253–2262, 2003.

[5] Valerio Lorenzoni and Daniele Ragni. Experimental investigation of the flow inside a saxophone mouthpiece by particle image velocimetry. *The Journal of the Acoustical Society of America*, 131(1):715–721, 2012.

[6] Yong Shi, Andrey R. da Silva, and Gary P. Scavone. LBM SIMULATION OF THE QUASI-STATIC FLOW IN A CLARINET. In *Proceedings of the Third Vienna Talk on Music Acoustics*, 2015.

[7] Andrey Ricardo da Silva, Gary P. Scavone, and Maarten van Walstijn. Numerical simulations of fluid-structure interactions in single-reed mouthpieces. *The Journal of the Acoustical Society of America*, 122(3):1798–1809, September 2007.

[8] Palabos. http://www.palabos.org/.

[9] Guillaume A. Brès, David Freed, Michael Wessels, Swen Noelting, and Franck Pérot. Flow and noise predictions for the tandem cylinder aeroacoustic benchmark. *Physics of Fluids*, 24(3):036101, March 2012.

[10] Federico Brogi, Orestis Malaspinas, Bastien Chopard, and Costanza Bonadonna. Hermite regularization of the lattice Boltzmann method for open source computational aeroacoustics. *The Journal of the Acoustical Society of America*, 142(4):2332–2345, 2017.

[11] Yu Hou, David Angland, Alois Sengissen, and Aline Scotto. Lattice-Boltzmann and Navier-Stokes Simulations of the Partially Dressed, Cavity-Closed Nose Landing Gear Benchmark Case. In *25th AIAA/CEAS Aeroacoustics Conference*, page 2555, 2019.

[12] E. W. S. Kam, R. M. C. So, and R. C. K. Leung. Lattice Boltzmann method simulation of aeroacoustics and nonreflecting boundary conditions. *AIAA journal*, 45(7):1703, 2007.

[13] Takaji Inamuro. Lattice Boltzmann methods for moving boundary flows. *Fluid Dynamics Research*, 44(2):024001, 2012.

[14] Orestis Malaspinas. Increasing stability and accuracy of the lattice Boltzmann scheme: Recursivity and regularization. *arXiv preprint arXiv:1505.06900*, 2015.

[15] Jonas Latt and Bastien Chopard. Lattice Boltzmann method with regularized pre-collision distribution functions. *Mathematics and Computers in Simulation*, 72(2-6):165–168, 2006.

[16] Christophe Coreixas, Gauthier Wissocq, Guillaume Puigt, Jean-François Boussuge, and Pierre Sagaut. Recursive regularization step for high-order lattice Boltzmann methods. *Physical Review E*, 96(3):033306, September 2017.

[17] A. R. da Silva, G. P. Scavone, and A. Lefebvre. Sound reflection at the open end of axisymmetric ducts issuing a subsonic mean flow: A numerical study. *Journal of Sound and Vibration*, 327(3):507–528, November 2009.

[18] Federico Avanzini and Maarten Van Walstijn. Modelling the mechanical response of the reed-mouthpiece-lip system of a clarinet. Part I. A one-dimensional distributed model. *Acta Acustica united with Acustica*, 90(3):537–547, 2004.

[19] Daniel Lagrava, Orestis Malaspinas, Jonas Latt, and Bastien Chopard. Advances in multi-domain lattice Boltzmann grid refinement. *Journal of Computational Physics*, 231(14):4808–4822, 2012.